

# THE DETERMINATION OF THE INCIDENT FLUX OF RADIO-METEORS

*T. R. Kaiser*

(Received 1960 April 7)

## *Summary*

The observed rate of radio-meteors depends on a number of factors which include: (i) the incident flux and distribution in magnitude of the meteors, (ii) the radiant co-ordinates, (iii) the variation in ionization along a meteor trail, (iv) the nature of the radio reflection process and (v) the parameters of the radio-echo equipment. The present work represents a considerable simplification over previous attempts (5, 6) to relate the radio echo rate to the actual flux of meteoroids. Simple formulae are derived relating these two quantities which, when used together with suitable graphical representation of the directional properties of the aerial system and of the reflection geometry, enable the incident flux of shower meteors to be deduced from the observed rate. The fact that the variation with time of the shower rate obtained with a fixed aerial beam may be predicted is relevant in connection with a method (7, 8) for shower radiant determination. Limitations due to the approximations in the theory, and to the simplified ablation theory on which it is based, are discussed.

---

1. *Introduction.*—The study of radio reflections from meteor trails has yielded a considerable amount of information concerning the properties and distribution of interplanetary matter and the physical processes accompanying the entry into the atmosphere of meteoric particles (meteoroids). A virtue of the technique is its inherent objectivity; the mechanism and geometry of reflection are fairly well understood and the essential equipment parameters (transmitted power, receiver sensitivity, aerial gain, etc.) are amenable to precise determination. It may therefore seem at first sight surprising that relatively little effort has been devoted to the problem of deducing the absolute incident flux of meteoroids from the observed echo rate. The following are the major difficulties which arise: (1) The reflection process is selective; echoes are only observed from trails which produce sufficient ionization in the vicinity of the specular reflection point (where a vector from the observer makes a normal intersection with the trail). (2) The sensitivity varies with direction in the aerial beam and with range. (3) In the case of sporadic meteors the relation between incident flux and echo rate depends on the orbital distribution. In view of the additional complication resulting from (3) the present discussion is limited to the case of shower meteors.

In former theoretical work (1, 2) concerned with the distribution of reflection points it was shown that they should be confined to a relatively narrow height interval about a mean height near 100 km and in spite of certain simplifying assumptions (particularly as concerns the meteor ablation process) fair agreement with observation has been obtained (3, 4). A previous extension of the theory to the present problem (5, 6) suffered through involving unduly complicated integrals which only in limiting cases (e.g. for a narrow, gaussian aerial beam)

led to manageable formulae. In the present work simple formulae are derived which combined with a suitable graphical procedure enable the magnitude distribution and incident flux of shower meteors to be derived from the observed echo rates. The theory enables the variation in echo rate due to the diurnal motion of the meteor radiant to be predicted and hence it has some importance in connection with the method for shower radiant determination developed by Clegg (7), particularly as modified by Keay (8) for high echo rates.

2. *The geometry of meteor reflections.*—On account of the specular condition all reflection points lie in the 'echo plane' ABCD (Fig. 1), which is normal to the radiant direction and passes through the observing station, O. The elevation of ABCD above the horizontal at O is thus equal to the radiant zenith distance,  $\chi_0$ , measured at O. The reflection points are further limited to a band corresponding to a relatively narrow height range about a mean height  $\bar{h}$  which defines the locus SS<sup>1</sup> in the figure (we will call SS<sup>1</sup> the 'echo line').

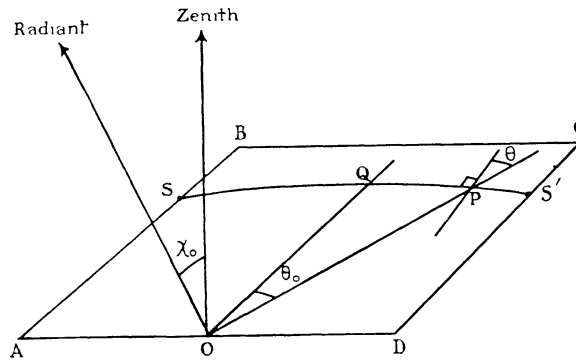


FIG. 1.—The echo plane ABCD which is normal to the radiant direction and contains the echo line SS<sup>1</sup>.

The minimum detectable line density,  $\alpha_P$ , in a meteor trail which intersects the echo plane at P is related to the system parameters by (5, 9, 10)\*.

$$\alpha_P = \left( \frac{32\pi^2 R^3 P_R}{P_T G \lambda^3} \right)^{1/2} \left( \frac{m c^2}{e^2} \right) \quad \text{for } \alpha_P < 2.4 \times 10^{12} \text{ cm}^{-1} \text{ (decay type echoes)} \quad (1)$$

and

$$\alpha_P = \left( \frac{54\pi^3 R^3 P_R}{P_T G \lambda^3} \right)^2 \left( \frac{m c^2}{e^2} \right) \quad \text{for } \alpha_P > 2.4 \times 10^{12} \text{ cm}^{-1} \text{ (persistent echoes)}. \quad (2)$$

Here,  $R = OP$ ,  $P_R$  = minimum detectable echo power,  $P_T$  = transmitted power,  $G = \sqrt{G_T G_R}$  where  $G_T$  and  $G_R$  are the transmitting and receiving aerial gains respectively,  $\lambda$  = wave-length,  $m$ ,  $e$ , and  $c$  are respectively the mass and charge of the electron and the velocity of light (in c.g.s. gaussian units).

From (1) and (2) we may deduce the variation in sensitivity for meteor detection, i.e. of  $\alpha_P$ , along the echo line SS<sup>1</sup>. However, since the echo plane moves through the aerial beam due to the daily motion of the radiant, it is more convenient to use the representation of Clegg (7) in which the contours of constant  $\alpha_P$  are plotted on a sphere (the 'echo surface') at height  $\bar{h}$  above the Earth's surface. This is illustrated in Fig. 2 for one of the rhombic aerials at

\* The echo enhancement due to plasma resonance (9) with transverse polarization has been ignored in (1). The numerical factor in (2) has been modified in accordance with a correction to the original theory due to Manning (11).

Sheffield with  $\bar{h}=100$  km. The projection is such that the radial coordinate is proportional to the distance  $R_S$  measured in the echo surface from its intersection with the observer's zenith; the normalized sensitivity contours are represented by lines of constant  $\rho=\alpha_{P0}/\alpha_P$ , where  $\alpha_{P0}$  is the minimum value of  $\alpha_P$  and depends on the equipment parameters as well as the aerial gain\*. The error in scaling distances in the curved echo surface directly from the projection of Fig. 2 is negligible.

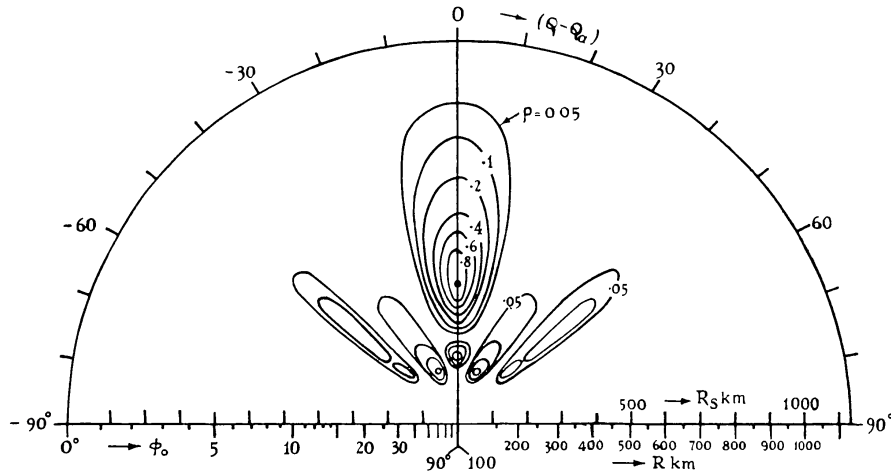


FIG. 2.—Normalized meteor sensitivity contours for one of the Sheffield rhombic aerials, projected onto the echo surface at 100 km height.  $R_S$ =radial distance measured in the echo surface from its intersection with the observer's zenith,  $R$ =slant range,  $\phi_0$ =elevation,  $\varphi$ =azimuth,  $\varphi_a$ =azimuth of beam axis (azimuths measured E of N).

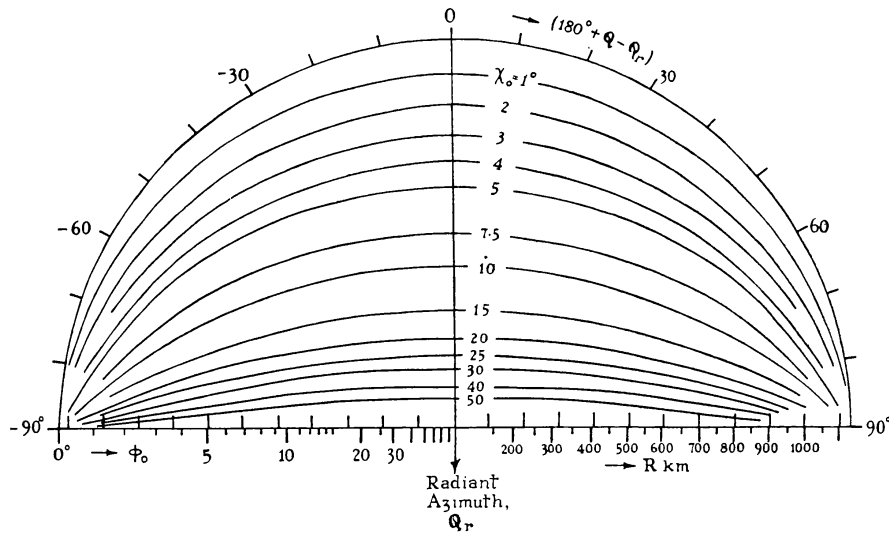


FIG. 3.—Echo lines on the 100 km echo surface (similar projection to Fig. 2).

The echo lines may also be represented on the echo surface as shown in Fig. 3. Given the radiant zenith distance ( $\chi_0$ ) and azimuth ( $\varphi_r$ ), Fig 3 can be superimposed on Fig. 2, and oriented so as to dispose correctly the radiant azimuth relative to that of the beam maximum, thus giving the intersection of the echo line with the sensitivity contours. In this way the variation of  $\alpha_P$  along an

\* Provided  $\alpha_{P0} \ll 10^{12}$  it is sufficient only to employ (1) in evaluating  $\rho$ , since in this case the contribution of persistent echoes to the total rate will be small.

echo line is obtained. The Geminid echo lines at various times relative to radiant transit are shown in Fig. 4 for an observer at Sheffield (latitude  $53^{\circ}23'$ )\*.

If the echo rate is sufficiently high, considerable simplification may be achieved by considering only echoes within a restricted range interval centred on some range  $R$  (e.g. the range at which  $\rho = 1$ ). In this case a set of curves of the type shown in Fig. 5 will be useful. These are loci of constant azimuth and zenith

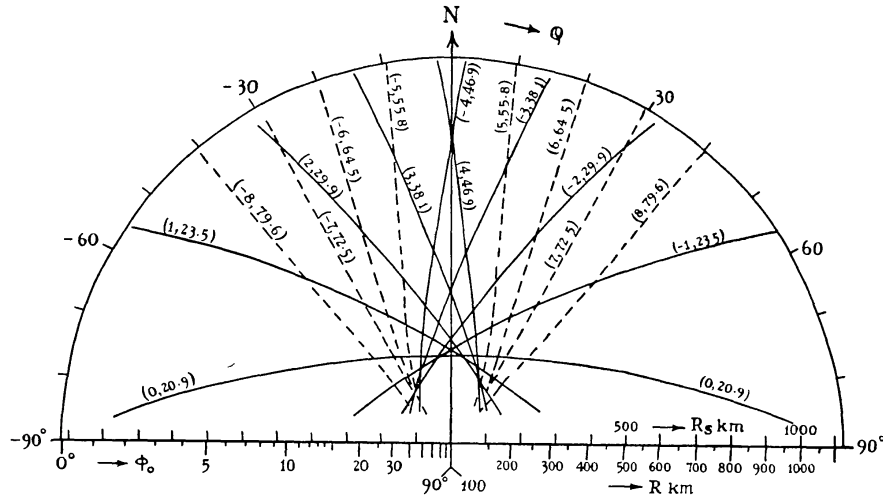


FIG. 4.—Geminid echo lines for the latitude of Sheffield ( $53^{\circ}23'N$ ) in a similar projection to Figs. 2 and 3. The figures on the curve are  $(T, \chi_0)$  where  $T$  hr. is the radiant hour angle and  $\chi_0$  degrees is the zenith distance.

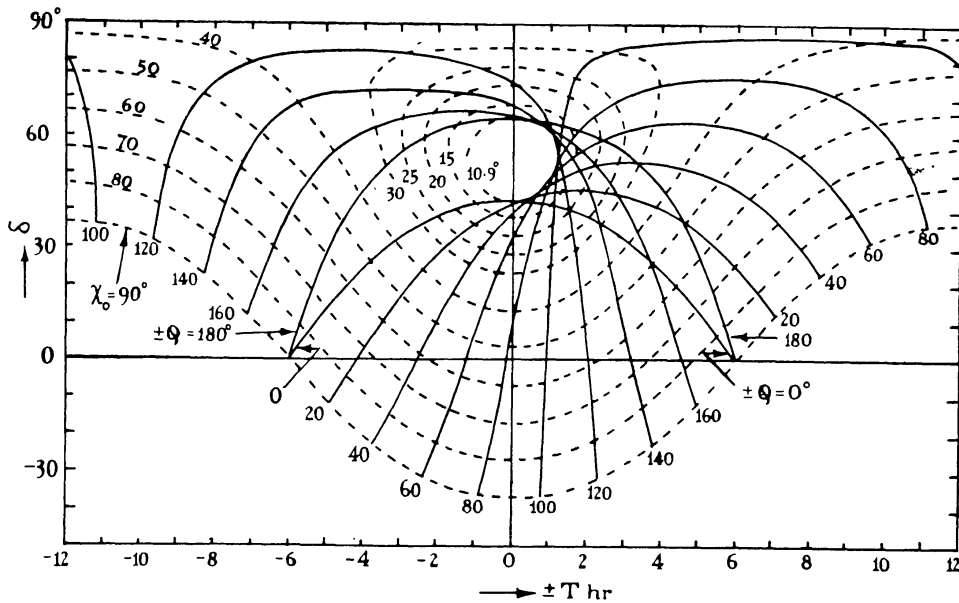


FIG. 5.— $T$  = hour angle at which the echo line for a radiant at declination  $\delta$  intersects azimuth  $\varphi(E$  of  $N)$  at slant range  $R = 450$  km ( $\phi_0 = 10.9^{\circ}$ , latitude  $53^{\circ}23'N$ ). The broken curves are loci of constant zenith distance,  $\chi_0$ .

distance of a point on the echo line at the fixed range  $R$ , plotted in radiant declination–hour angle coordinates. Given a set of such curves, together with the sensitivity contours of Fig. 2, the sensitivity factor  $\rho$  and zenith distance  $\chi_0$

\* Formulae relating  $\chi_0$  and  $\varphi_T$  to the celestial coordinates of the radiant and for calculating the echo lines in the projection of Fig. 3 are given in the Appendix.

can be determined as a function of hour angle for any specified radiant declination. In particular the time at which the echo line intersects the point of maximum sensitivity (on the beam axis) is easily ascertained. A method for computing these curves will be found in the Appendix.

3. *The representation of the incident flux of shower meteors.*—An approximate relation for the electron line density  $\alpha$  cm<sup>-1</sup> produced by a spherical meteoroid travelling through a rarefied isothermal atmosphere is (12):

$$\alpha = \alpha_m (p/p_m) (1 - \frac{1}{3} p/p_m)^2 \quad (3)$$

where the maximum line density  $\alpha_m$  occurs at pressure  $p_m$ ;  $\alpha_m$  is proportional to the initial mass of the meteoroid and to  $\cos \chi$ . If the pressures  $p$ ,  $p_m$  occur at heights  $h$ ,  $h_m$ , then

$$h - h_m = H \ln (p/p_m) \quad (4)$$

where  $H$  is the exponential scale height. (3) and (4) define the line density as a function of height (Fig. 6). Weiss (13) has obtained a more exact equation and has considered the effect of a linear height gradient of  $H$ . However in neither case is the form of the electron density profile altered to an extent which would be serious for the present purposes. Indeed major departures from the simple ablation theory are more likely to come from processes such as fragmentation (14).

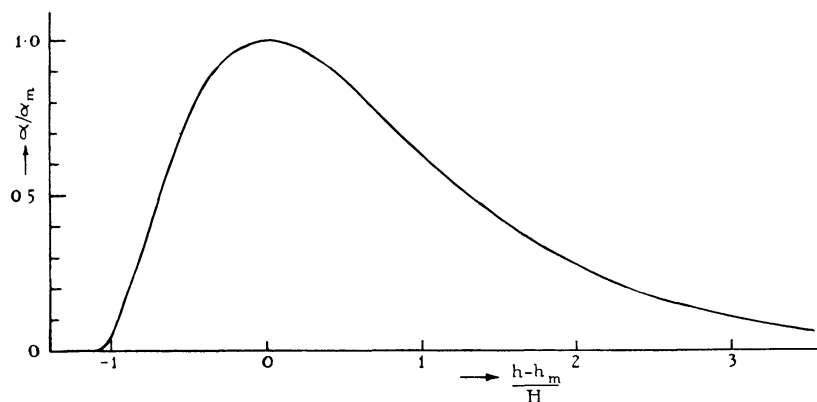


FIG. 6.—Meteor ionization profile.

In view of the dependence of  $\alpha_m$  on  $\chi$  it is convenient to introduce the quantities

$$\alpha_z = \alpha_m (\cos \chi)^{-1} \quad (5)$$

which we will call the maximum “zenithal” line density (i.e. the line density which the meteoroid would produce if incident vertically) and the absolute radio magnitude  $M$  which is defined by Kaiser (10) as

$$M = -2.5 \log_{10} \alpha_z + 35. \quad (6)$$

Decay type echoes occur for  $M > +5$

The incident flux of meteoroids (per unit time across unit area normal to the radiant direction) can thus be represented by:

$\Phi(\alpha_z) d\alpha_z$  = flux producing zenithal line densities between  $\alpha_z$  and  $\alpha_z + d\alpha_z$ ,

$\Theta(\alpha_z)$  = flux producing zenithal line densities greater than  $\alpha_z$ ,

$A(M) dM$  = flux producing meteors with magnitude between  $M$  and  $M + dM$ ,

$B(M)$  = flux producing meteors brighter than magnitude  $M$ .

In many cases we can approximate to the distribution function  $\Phi$  by the power law

$$\Phi(\alpha_z) = c\alpha_z^{-s} \quad (7)$$

where  $c$  and  $s$  are constants. Such a law appears to hold for sporadic meteors over a wide range of magnitudes with  $s$  close to 2.0 (2, 5). In a study of the major showers (6)  $s$  was found to have some dependence on  $\alpha_z$  and to be generally less than 2, at least for the sub-visual radio meteors. If (7) is valid we obtain:

$$\Theta(\alpha_z) = \frac{c}{(s-1)\alpha_z^{s-1}} \quad (8)$$

and

$$B(M) \propto A(M) \propto a^M \quad (9)$$

where  $s = 1 + 2.5 \log a$ . For  $s = 2$  we get  $a = 2.51$  which corresponds to a constant total mass of meteoric material per unit magnitude interval.

4. *The echo rate per unit length of echo line.*—With the help of the geometrical considerations in Section 2 we can now relate the observed shower echo rate to the actual incident flux of meteoroids.

Consider those meteoroids incident upon a strip of the echo plane at P (Fig. 1) which is normal to the echo line and is of width  $dl$ , and let the height and atmospheric pressure at burn-out be  $h_0$  and  $p_0$  respectively. Equation (3) may thus be re-written:

$$\alpha/\alpha_m = \frac{27}{4} u(1-u)^2 \quad (10)$$

where  $u = p/p_0 = \exp(-x/H)$ ,  $x = h - h_0$ . The number of meteors passing through the interval of the strip between heights  $x$  and  $x + dx$  above  $h_0$  and with maximum line densities in excess of  $\alpha_m$  is simply

$$dN = \Theta \left( \frac{\alpha_m}{\cos \chi} \right) \frac{dl dx}{\sin \chi}. \quad (11)$$

The radio-echoes from these will be detected provided the line density at the echo plane is in excess of  $\alpha_p$ , i.e. provided\*

$$\alpha_m \geq \frac{4}{27} \alpha_p u^{-1}(1-u)^{-2}. \quad (12)$$

The total number of echoes obtained from meteors intersecting the strip is therefore

$$N_1 dl = \frac{H dl}{\sin \chi} \int_0^1 \Theta(\alpha_{zx}) \frac{du}{u}. \quad (13)$$

Where  $\alpha_{zx} = \frac{4}{27} \frac{\alpha_p}{\cos \chi} u^{-1}(1-u)^{-2}$ ; it is the maximum zenithal line density of the faintest detectable meteor at height  $h_0 + x$ . Thus  $N_1$  is the observed echo rate per unit length of echo line.

\* If the height interval from which echoes are obtained is reasonably small compared with the mean height  $\bar{h}$  we can treat the minimum detectable line density as constant over the strip and equal to its value  $\alpha_p$  on the mean echo line.

If  $\Theta(\alpha_z)$  can be represented by equation (8) we get the simple result:

$$N_1 = \frac{HI}{\sin \chi} \Theta\left(\frac{\alpha_P}{\cos \chi}\right) \quad (14)$$

where

$$I = \left(\frac{27}{4}\right)^{s-1} \int_0^1 u^{s-2} (1-u^2)^{s-1} du = \left(\frac{27}{4}\right)^{s-1} \frac{\Gamma(s-1)\Gamma(2s-1)}{\Gamma(3s-2)} \quad (15)$$

and is plotted in Fig. 7.

$HI$  is simply the area of the normalized distribution in height of the reflecting points in the strip of the echo plane and  $I$  is identical with the integral

$$I_1 = \int_{-\infty}^{\infty} \left[ \frac{3e^x}{2e^{3x/2} + 1} \right]^{3(s-1)} dx$$

which appears in earlier work (1, 2, 5, 6).  $HI/\cos \chi$  may be regarded as an average effective length of the trails of radio-meteors.

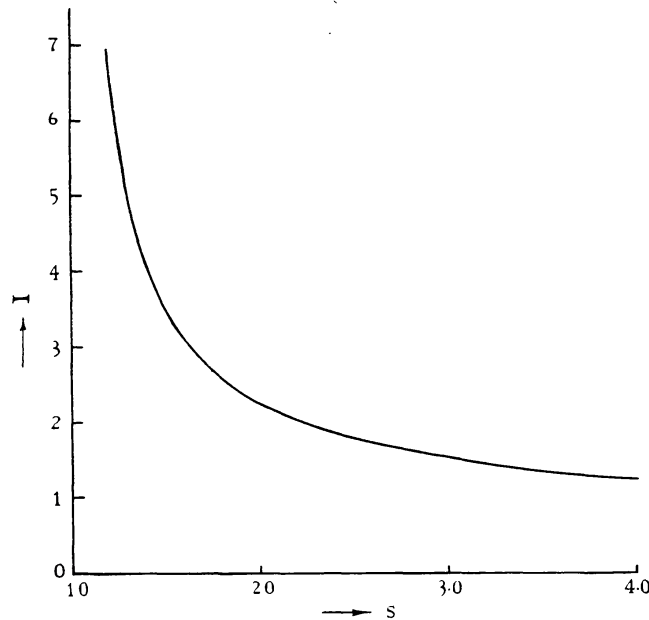


FIG. 7.— $I = \left(\frac{27}{4}\right)^{s-1} \int_0^1 u^{s-2} (1-u^2)^{s-1} du$ .

The zenith distance  $\chi$  in the above is the value at the point P on the echo line and it differs from the value  $\chi_0$  at the observer. To a close approximation we may substitute (see Appendix):

$$\cos \chi \simeq \cos \chi_0, \quad \sin^2 \chi \simeq \sin^2 \chi_0 + 2\bar{h}/R_E$$

where  $R_E$  is the Earth's radius, whence we obtain

$$N_1 = Hf_1(\chi_0, s)\Theta(\alpha_P) \quad (16)$$

where

$$f_1(\chi_0, s) = I(\cos \chi_0)^{s-1} (\sin^2 \chi_0 + 2\bar{h}/R_E)^{-1/2}. \quad (17)$$

$f_1(\chi_0, s)$  is given in Fig. 8 as a function of  $\chi_0$  for a range of values of  $s$  (with  $\bar{h} = 100$  km).

Using the method of Section 2, the sensitivity factor  $\rho$  may be determined at all points along the echo line, hence the echo rate  $N$  over part or the whole of the echo line can be obtained, by numerical integration, from

$$N = Hf_1(\chi_0, s) \Theta(\alpha_{P0}) \int \rho^{s-1} dl. \quad (18)$$

The echo rate between specific range limits can be found by evaluating the integral in (18) along the appropriate intercept of the echo line.

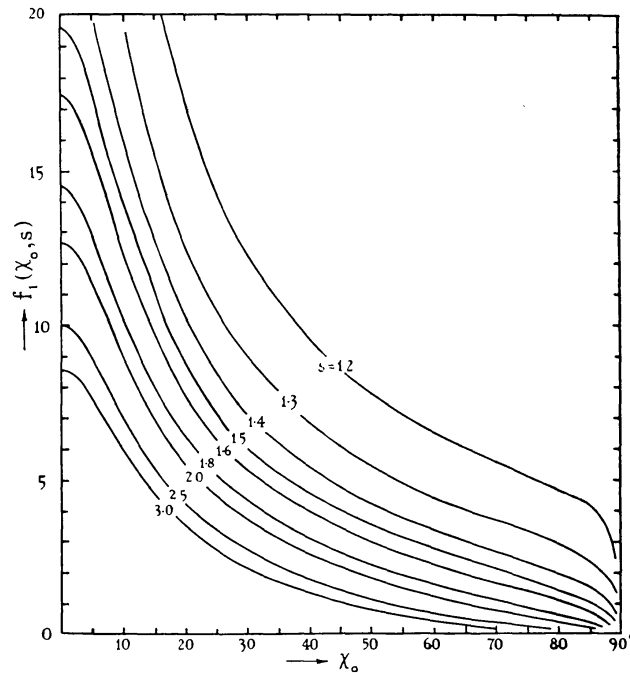


FIG. 8.—The rate factor  $f_1(\chi_0, s)$  as a function of  $\chi_0$  for various  $s$  ( $\bar{h} = 100$  km).

The value of  $s$  can be found from the distribution in amplitude of the shower meteor echoes or from the dependence of echo rate on equipment sensitivity (5, 6, 15). By substituting it into (18) we obtain the factor relating  $N$  to  $\Theta$  and hence the incident flux may be deduced from the observed echo rate.

5. *The echo rate per unit range interval.*—In Fig. 1,  $\theta$  is the angle between OP and the normal to the echo line at P.  $\phi, \phi_0$  are the elevation of OP above a horizontal plane at P and O respectively.  $\theta_0$  is the angle QOP where OQ is the intersection between the echo plane and the plane through O, the zenith and radiant point.

We have  $\sin \theta = dR/dl$  where  $dR$  is the range interval corresponding to the element  $dl$  of the echo line. Thus if  $N_2 dR$  is the rate of echoes with ranges between  $R$  and  $R + dR$  we obtain, using (14),

$$N_2 = \frac{HI}{\sin \theta \sin \chi} \Theta \left( \frac{\alpha_P}{\cos \chi} \right). \quad (19)$$

To a sufficient order of approximation (see Appendix),

$$\sin \theta \sin \chi \simeq \sqrt{(\sin^2 \chi_0 - \sin^2 \phi_0)}, \quad \cos \chi \simeq \cos \chi_0,$$

hence

$$N_2 = Hf_2(\chi_0, s)\Theta(\alpha_p) \quad (20)$$

where

$$f_2(\chi_0, s) = I(\cos \chi_0)^{s-1} (\sin^2 \chi_0 - \sin^2 \phi_0)^{-1/2}; \quad (21)$$

$N_2$  depends on  $R$  through  $\sin \phi_0 \simeq \frac{\bar{h}}{R} - \frac{R}{2R_E}$ .

Equation (20) gives the rate per unit range; it can be applied to a finite range interval provided the sensitivity factor  $\rho$  does not vary appreciably along the intercept of echo line. It clearly fails when  $\phi_0$  approaches  $\chi_0$ , when the echo line becomes tangent to the circle of constant range  $R$  (i.e. when P and Q in Fig. 1 coincide). In this case we must revert to the method of Section 4 and evaluate the integral of  $\rho^{s-1}$  along the echo line (for the result to be valid the range interval must be sufficiently large to encompass the range spread due to the finite dispersion in height of the reflection points). In this manner the mean rate  $\bar{N}$  between 400 and 500 km has been evaluated, for echo lines intersecting the beam axis of the Sheffield rhombics at range 450 km\*. The result is illustrated in Fig. 9 where the full curves give  $\bar{N}/[H\Theta(\alpha_{p0})] = \bar{f}_2(\chi_0, s)$ ; they may be compared with  $f_2(\chi_0, s)$  evaluated for  $R = 450$  km, given as broken curves.

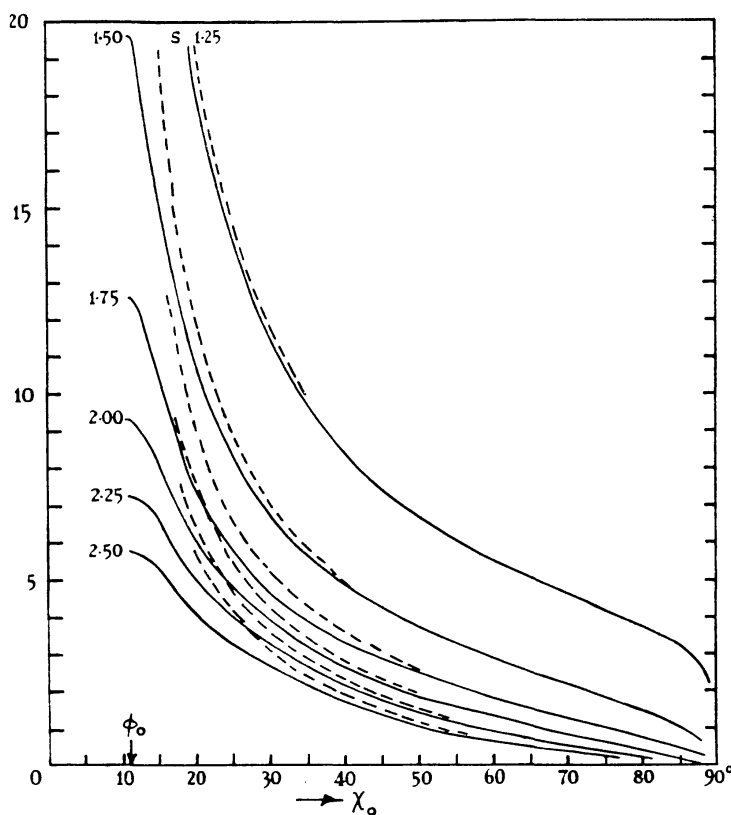


FIG. 9

—  $\bar{f}_2(\chi_0, s)$  evaluated for the Sheffield rhombic aerials with  $400 < R < 500$  km.  
 - - -  $f_2(\chi_0, s)$  for  $R = 450$  km ( $\phi_0 = 10.9^\circ$ ).

6. *The determination of shower radiants.*—The method of Clegg (7) and its modification due to Keay (8) rests essentially on the assumption that the

\* This will be approximately the condition for maximum rate per unit range at  $R = 450$  km (but see Section 6).

maximum shower echo rate at a given range occurs when the echo line intersects the beam axis at that range. Referring to Fig. 5 we see that the radiant declination and right ascension can be estimated from the times of maximum rate on two aerials at different azimuths. It is clear from the above, however, that the zenith distance will be changing as the echo line moves through the beam causing a displacement in the time of maximum rate which will occur earlier or later depending upon whether  $\chi_0$  is an increasing or decreasing function of  $T$ . The magnitude of the displacement will depend, *inter alia*, on the azimuthal width of the aerial beams (being greater, the wider the beam) and on the radiant declination. It is clear that the present theory enables these time displacements to be estimated and appropriate corrections to be made.

7. *An alternative approach to the problem.*—If we consider again a narrow strip in the echo plane, normal to the echo line at P, we see that a meteor trail with maximum line density  $\alpha_m$  can be detected over a height range  $H \ln(u_1/u_2)$  where  $u_1, u_2$  ( $u_1 > u_2$ ) are the positive solutions of the cubic equation (10) with  $\alpha = \alpha_p$ . The quantity  $\ln(u_1/u_2)$  is thus a function of  $\alpha_m$  (for given  $\alpha_p$ ) and may be regarded as a weighting factor which when multiplied by the differential distribution function  $\Phi(\alpha_m/\cos \chi)$  gives the distribution of maximum line densities of the meteor trails which are actually observed (see Fig. 10).

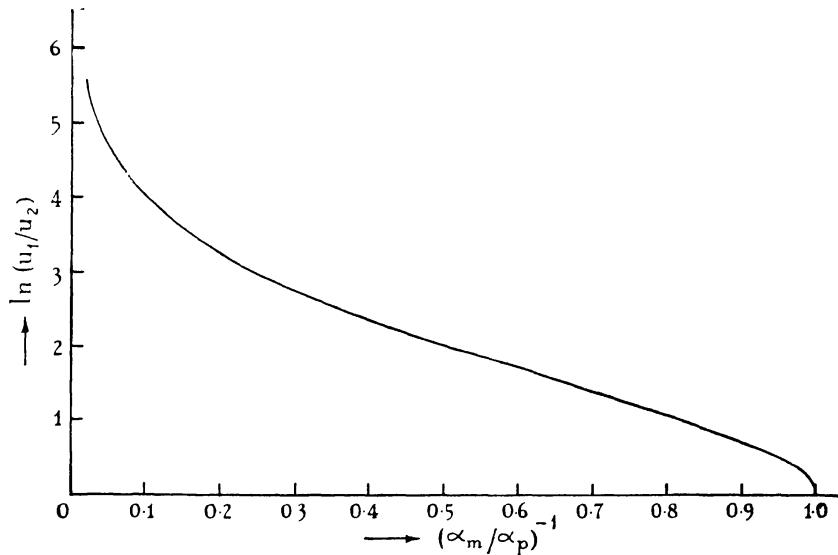


FIG. 10

Thus the number of echoes observed per unit length of echo line at P from meteors with line densities between  $\alpha_m$  and  $\alpha_m + d\alpha_m$  is  $n(\alpha_m) d\alpha_m$  where

$$n(\alpha_m) = \frac{H}{\sin \chi \cos \chi} \ln \frac{u_1}{u_2} \Phi \left( \frac{\alpha_m}{\cos \chi} \right). \quad (22)$$

For the special case when  $\Phi$  may be represented by the power law we get

$$n(\alpha_m) \propto z^{-s} \ln(u_1/u_2) \quad (23)$$

where  $z = \alpha_m/\alpha_p$ . When  $z \gg 1$ ,  $u_1/u_2 \simeq 27z/4$ . Fig. 11 illustrates how  $n(\alpha_m)$  from (23) varies with  $\alpha_m$ . For  $s=2$  the most frequently observed meteor has maximum line density about 1.3 times the threshold value,  $\alpha_p$ .

The total observed rate per unit length of echo line, for any distribution  $\Phi$  is obtained by integrating (22) giving

$$N_1 = \frac{H\alpha_P}{\sin \chi \cos \chi} \int_1^\infty \ln \frac{u_1}{u_2} \Phi \left( \frac{z\alpha_P}{\cos \chi} \right) dz. \quad (24)$$

Equation (24) enables the observed rate to be predicted if  $\Phi$  is known but unfortunately it is of little value in deducing  $\Phi$  from the observations. It is nevertheless instructive in showing that only for the power law does  $N_1$  have the same functional dependence as  $\Theta$  on the limiting line density,  $\alpha_P$ ; in this case (24) becomes

$$N_1 = \frac{(s-1)H}{\sin \chi} \Theta \left( \frac{\alpha_P}{\cos \chi} \right) \int_1^\infty z^{-s} \ln(u_1/u_2) dz. \quad (25)$$

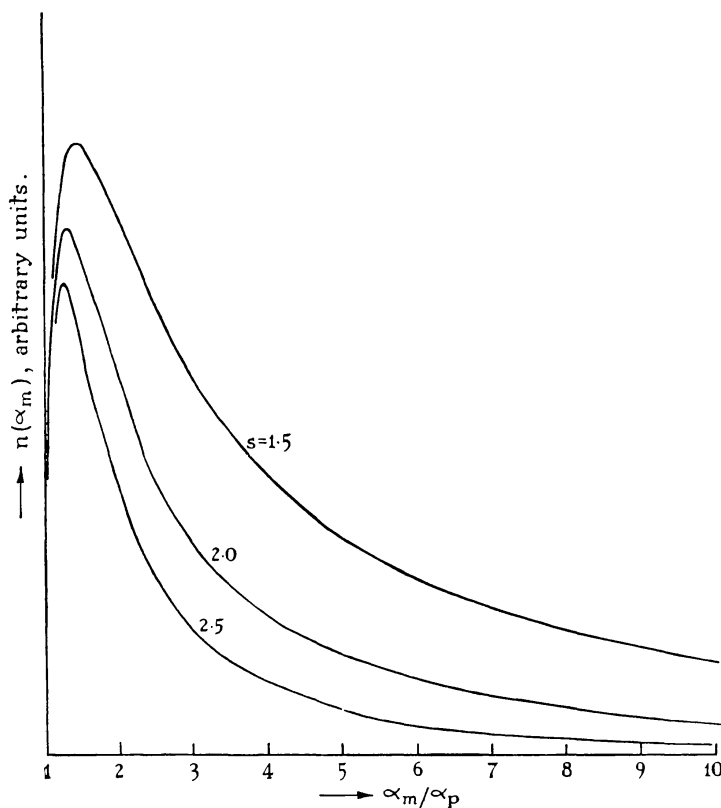


FIG. 11.—Differential distribution in maximum electron line density of observed meteors for an incident distribution satisfying an inverse power law with exponent  $s$ .

8. *Discussion.*—A number of approximations have been made in order to secure the simplest procedure for deducing the incident flux of meteoroids from the observed radio-echo rates. To whatever extent this may limit the absolute accuracy of the result, the above treatment should prove of considerable value for comparison of the incident fluxes and magnitude distributions in the various meteor showers.

Errors will clearly result if the ablation process deviates from the theoretical model; for instance if the phenomenon of fragmentation (14) is important for the faint radio-meteors the factor  $HI$  in the echo rate equations will be an overestimate. Rapid diffusion of meteor trails will limit the height to which they can be observed, particularly on short wave-lengths, while on longer wave-lengths

( $\lambda > 15\text{m}$ ) ionospheric D-region absorption and Faraday rotation may at times have a significant effect on the rate (Baldwin and Kaiser (unpublished) have observed a marked decrease in the echo rate on 17 Mc/s associated with a short-wave radio fade-out). The effects of rapid diffusion will be most marked for fast meteors (which tend to ionize at greater heights) and for showers with values of  $s$  markedly less than 2, when the theory predicts a substantial proportion of echoes from meteors considerably brighter than the threshold for detection (and which may therefore be seen to greater heights).

Deviation of the distribution of maximum line densities from the simple power law with constant exponent  $s$  will lead to error since it was shown in Section 7 that only in this case does the echo rate have the same functional dependence as  $\Theta$  on  $\alpha_p$ . Observations of sporadic meteors made at Sheffield (unpublished) give  $s$  near to 2.0 down to 11th radio magnitude, with no significant seasonal or diurnal variation. However, considerable deviations from a power law are found in the case of a number of meteor showers. In these cases the exponent deduced from the variation of echo rate with equipment sensitivity (or from the echo amplitude distribution) will be close to the true value only if  $s$  varies sufficiently slowly with  $\alpha_z$ , this condition being more stringent the smaller the value of  $s$ . In fact, provided  $s$  is not too small, most observed meteors will have magnitudes near to the limit of detection in which case the threshold value of  $s$  may be used in the echo rate equations without serious error.

It has been assumed that the echoes all originate in a narrow band about a mean height  $\bar{h}$  (which will tend to be higher the larger the meteor velocity and the more sensitive the apparatus) and that the limiting sensitivity is constant across this band. In fact the minimum detectable line density will tend to increase with height across the echo band (due to increased range) and this will again cause the present theory slightly to overestimate the echo rate. The representation of the echo band by a mean echo line on a constant height surface introduces an additional limitation since the echoes corresponding to the point P on this line will actually be spread in range over an interval  $\Delta R$  where

$$\Delta R \sim HI (\sin \phi)^{-1} \simeq HI (\sin^2 \phi_0 + 2h/R_E)^{-1/2}.$$

This will not be serious provided (a) the sensitivity factor  $\rho$  does not vary substantially over the range interval  $\Delta R$  and (b) that if  $\chi_0$  approaches  $\phi_0$  the range interval within which the echoes are counted is at least a few times  $\Delta R$ .

It has been further supposed that the shower has a well defined point radiant. A spread in the radiant will not be serious provided it is reasonably small compared with the aerial beam width, except when  $\chi_0$  approaches  $\phi_0$  when the range interval needs to be large enough to encompass any additional range spread due to the finite radiant area.

A final difficulty can arise in subtracting the sporadic rate from the total in order to obtain the shower rate. Since  $s$  is generally smaller for shower than for sporadic meteors the ratio (shower rate : sporadic rate) decreases with increasing equipment sensitivity (increasing total rate) until eventually the shower may be scarcely observed against the sporadic background. In these cases it may be difficult to estimate shower rates unless some method for selecting shower meteors (e.g. by velocity) is used to distinguish them from the background.

## APPENDIX

(i) *Transformation of the radiant coordinates.*

Let

- $l$  = latitude of observer,  
 $\delta$  = radiant declination,  
 $T$  = radiant hour angle,  
 $\varphi_r$  = radiant azimuth (E of N),  
 $\chi_0$  = radiant zenith distance.

A convenient form for the solution to the astronomical triangle is

$$f(\chi_0) - \sin \chi_0 (1 - \cos \varphi_r) = f(\delta - l) \quad (26)$$

where

$$f(x) = \sin x + \tan l \cos x.$$

Given the latitude  $l$ ,  $f(x)$  may be presented in tabular or graphical form and used to evaluate  $\delta$  for any given  $\chi_0$ ,  $\varphi_r$ . The hour angle can then be obtained from either of the relations

$$\sin T = - \frac{\sin \chi_0 \sin \varphi_r}{\cos \delta} \quad (27)$$

or

$$\cos T = \frac{\cos \chi_0 - \sin l \sin \delta}{\cos l \cos \delta}. \quad (28)$$

(ii) *Equations for the echo line*

If  $\phi_0$ ,  $\varphi$  are the elevation and azimuth from O of the point P on the echo line (Fig. 1) then it can be shown that

$$\tan \phi_0 = - \tan \chi_0 \cos (\varphi_r - \varphi). \quad (29)$$

The slant range  $R$  and the curved distance  $R_s$  (see Fig. 12) are related to  $\phi_0$  through

$$R \simeq R_E \left( \sqrt{\sin^2 \phi_0 + \frac{2\bar{h}}{R_E}} - \sin \phi_0 \right) \quad (30)$$

and

$$R_s \simeq R \cos \phi_0 \quad (31)$$

where  $R_E$  is the Earth's radius.

Equations (29), (30), (31) give the coordinates ( $R_s$ ,  $\varphi$ ) of the point P on the echo line for any given zenith distance  $\chi_0$ . They have been used for the construction of Fig. 3.

(iii) *Equations for the curves of Fig. 5*

We wish to determine the radiant hour angle when the echo line corresponding to a radiant at declination  $\delta$  intersects a point on the echo surface at azimuth  $\varphi$  and slant range  $R$ .  $R$  is related to  $\phi_0$  by (30) and  $\varphi$  is obtained as a function of  $\phi_0$  from (29).  $\delta$  is then obtained as a function of  $T$  through the procedure in (i) (note that  $\chi_0 \geq \phi_0$ ).

(iv) Relations between  $\phi$ ,  $\phi_0$ ,  $\chi$ ,  $\chi_0$ ,  $\theta$  (see Sections 4, 5)

Consider the triangle OPC (Fig. 12) where C is the centre of the Earth. It will be recalled that  $\phi$  is the elevation of OP above the horizontal at P, thus the angle OPC is equal to  $\pi/2 - \phi$  and we obtain

$$\frac{\cos \phi_0}{\cos \phi} = 1 + \frac{h}{R_E} \simeq 1 \quad (32)$$

from which it follows that

$$\sin^2 \phi \simeq \sin^2 \phi_0 + \frac{2h}{R_E}. \quad (33)$$

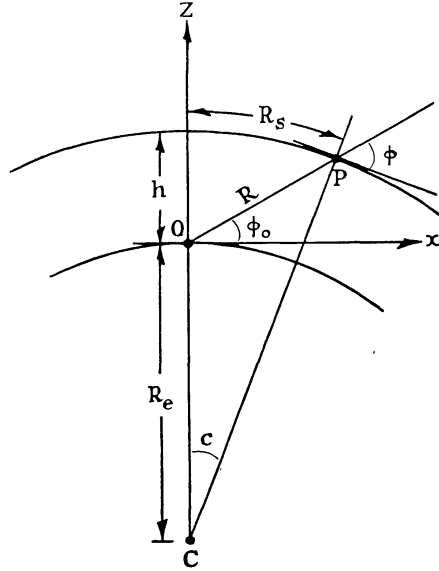


FIG. 12

In the right-handed coordinate system  $Oxz$  of Fig. 12, let the radiant have direction cosines  $(l, m, n)$  where  $n = \cos \chi_0$ . The direction cosines of  $OP$  and  $CP$  are  $(\cos \phi_0, 0, \sin \phi_0)$  and  $(\sin c, 0, \cos c)$  respectively. Now  $\chi$  is the radiant zenith distance at  $P$ , hence

$$\cos \chi = l \sin c + \cos \chi_0 \cos c$$

and since the radiant direction is normal to  $OP$ ,

$$0 = l \cos \phi_0 + \cos \chi_0 \sin \phi_0.$$

Eliminating  $l$  from the above two equations, and putting  $\phi = \phi_0 + c$ , we get

$$\left. \begin{aligned} \frac{\cos \chi_0}{\cos \chi} = \frac{\cos \phi_0}{\cos \phi} = 1 + \frac{h}{R_E} \simeq 1 \\ \sin^2 \chi \simeq \sin^2 \chi_0 + \frac{2h}{R_E}. \end{aligned} \right\} \quad (34)$$

and

Referring to Fig. 1 we see that  $\sin \chi \cos \theta = \sin \phi$ , whence, using (34), we obtain

$$\sin \chi \sin \theta = \left(1 + \frac{h}{R_E}\right)^{-1} \sqrt{(\sin^2 \chi_0 - \sin^2 \phi_0)}. \quad (35)$$

The University,  
Sheffield:  
1960 April.

*References*

- (1) Kaiser, T. R., *M.N.*, **114**, 39, 1954.
- (2) Kaiser, T. R., *M.N.*, **114**, 52, 1954.
- (3) Evans, S., *M.N.*, **114**, 63, 1954.
- (4) Weiss, A. A., *Aust. J. Phys.*, **12**, 54, 1959.
- (5) Kaiser, T. R., *Adv. Phys. (Phil. Mag. Supp.)*, **2**, 495, 1953.
- (6) Kaiser, T. R., " *Meteors* " ed. T. R. Kaiser (Pergamon Press: London), p. 119, 1955.
- (7) Clegg, J. A., *Phil. Mag.*, **34**, 577, 1948.
- (8) Keay, C. S. L., *Aust. J. Phys.*, **10**, 471, 1957.
- (9) Kaiser, T. R., and Closs, R. L., *Phil. Mag.*, **43**, 1, 1952.
- (10) Kaiser, T. R., " *Meteors* " ed. T. R. Kaiser (Pergamon Press: London), p. 55, 1955.
- (11) Manning, L. A., *J. Atmos. Terr. Phys.*, **4**, 219, 1953.
- (12) Herlofson, N., *Phys. Soc. Rep. Prog. Phys.*, **11**, 444, 1948.
- (13) Weiss, A. A., *Aust. J. Phys.*, **11**, 591, 1958.
- (14) Jacchia, L. G., " *Meteors* " ed. T. R. Kaiser (Pergamon Press: London), p. 36, 1955.
- (15) Browne, I. C., Bullough, K., Evans, S., and Kaiser, T. R., *Proc. Phys. Soc.*, B **69**, 83, 1956.